

1 **A new joint optimization method for design and operation of multi-**
2 **reservoir system considering the conditional value-at-risk**

3

4 Xiaoqi Zhang^{a,b,c,d}, Pan Liu^{c,d*}, Maoyuan Feng^{c,d}, Chong-Yu Xu^e, Lei Cheng^{c,d}, Yu
5 Gong^{c,d}.

6

7 ^a Changjiang River Scientific Research Institute, Changjiang Water Resources
8 Commission of the Ministry of Water Resources of China, Wuhan 430010, China

9 ^b Hubei Key Laboratory of Water Resources & Eco-Environmental Sciences,
10 Changjiang River Scientific Research Institute, Wuhan 430010, China

11 ^c State Key Laboratory of Water Resources and Hydropower Engineering Science,
12 Wuhan University, Wuhan 430072, China

13 ^d Hubei Provincial Key Lab of Water System Science for Sponge City Construction,
14 Wuhan University, Wuhan 430072, China.

15 ^e Department of Geosciences, University of Oslo, PO Box 1047 Blindern, 0316 Oslo,
16 Norway

17

18 Corresponding author: Pan Liu

19 E-mail address: liupan@whu.edu.cn.

20 Tel.: +86 27 68775788; Fax: +86 27 68773568.

21 **Abstract:**

22 The joint design and operation of multi-reservoir systems is a vital issue for reservoir
23 management. Existing studies mostly focus on determining the optimal scheme by
24 establishing an optimization model and relying on intelligent algorithms. However, the
25 research on the mutual feedback mechanism between the flood control capacity of each
26 reservoir has not been adequately addressed. The overall aim of this paper is to propose
27 a new joint optimization method for design and operation of multi-reservoir systems
28 considering the conditional value-at-risk ($CVaR_\alpha$). In the proposed method, the flood
29 damage assessment with $CVaR_\alpha$ for a multi-reservoir system is constructed firstly,
30 and then the feasible flood storage combination scheme (FSCS) of reservoirs in the
31 system is deduced. Finally, the tradeoffs between the hydropower generation benefit
32 and flood damage loss have been analyzed. Selecting China's Ankang-Danjiangkou
33 Cascade Reservoirs as a case study, the results indicate that (1) the $CVaR_\alpha$ value is
34 more sensitive to changes in the flood storage of Danjiangkou reservoir (larger and
35 downstream) than that of Ankang reservoir (smaller and upstream); (2) the feasible area
36 of the FSCSs can be described as a triangle, and the boundary of this feasible interval
37 is determined by the allowable minimum flood storage (AMFS) value of each reservoir;
38 and (3) the relationship between the hydropower generation benefit and the flood
39 damage assessment index $CVaR_\alpha$ is not monotonic. These findings are helpful for
40 understanding the relationship between flood storage values of each reservoir from the
41 perspective of the entire multi-reservoir system.

- 42 **Keywords:** Joint design operation; Multi-reservoir system; Flood storage; Conditional
- 43 value-at-risk; Flood damage assessment.

44 **1. Introduction**

45 The joint design and operation of multi-reservoir systems is a necessary technical
46 practice to realize the safe and efficient utilization of flood resources (Dogan Mustafa
47 et al., 2021; Ming et al., 2021; Yeh, 1985; Yun and Singh, 2008; Zhou et al., 2018) when
48 facing the increase in the dimension of the coordinated flood control reservoirs (Cheng
49 et al., 2021; He et al., 2019). Specifically, the flood limited water level (FLWL), which
50 corresponds to the reservoir flood storage value, is a vital parameter for controlling the
51 trade-offs between operation objectives of flood control and water conservation (Jiang
52 et al., 2015; Liu et al., 2015a). In China, the FLWL is usually determined by flood
53 routing of design floods under the condition that the flood prevention risk does not
54 increase (Liu et al., 2015b; Zhang et al., 2018). However, the traditional design method
55 for the flood storage is separately derived from the perspective of each individual
56 reservoir, and is not intended to maximize the benefits for the entire multi-reservoir
57 system. Therefore, the joint design method of deriving optimal flood storage
58 combination scheme (FSCS) for multi-reservoir systems should be developed.

59 Many researchers have already focused on the joint optimal design of the flood
60 storage values for the complex multi-reservoir systems (Gong et al., 2020; Tan et al.,
61 2017). Chen et al. (2012) deduced the feasible interval of the reservoir flood storage in
62 a multi-reservoir system by establishing a composition and decomposition-based model,
63 which consists of an aggregation module, a storage decomposition module and a
64 simulation operation module. Zhou et al. (2014) described a joint operation and

65 dynamic control model of FLWL for a mixed reservoir system, and improved the
66 hydropower benefit and the water resource utilization without reducing the originally
67 designed flood prevention standards. Hui and Lund (2015) proposed a flood storage
68 allocation model for parallel reservoirs with the objective of minimizing the
69 downstream damage caused by the possible high peak flow of the upper stream
70 reservoirs. Ouyang et al. (2015) presented a multi-objective optimal design model for
71 FLWLs of multi-reservoir system, which can make better use of water resources
72 without increasing the flood control risk. However, previous studies mostly focus on
73 determining the optimal scheme by establishing an optimization model and relying on
74 intelligent algorithms, which are lack of identifying the mutual feedback mechanism
75 between the flood control capacity of each reservoir.

76 Recently, the response relationship between the individual reservoir's flood
77 storage and its benefit (which mainly refers to hydropower generation and water supply)
78 has been studied by a large number of researchers, and the law of feedback mechanism
79 can be summarized as follows (Dogan et al., 2021): the hydropower generation or water
80 supply benefit of the single reservoir system shows a monotonous correlation with the
81 reservoir flood storage value, that is, the larger the flood storage value is, the greater
82 the flood control capacity (the lesser the hydropower generation or water supply benefit)
83 is. However, the above regular pattern is not applicable to the multi-reservoir system
84 because of the complex hydrological and hydraulic connection between the reservoirs

85 in the system. The impact on the overall benefit of the multi-reservoir system caused
86 by one of reservoirs' flood storage is uncertain, and then the maximization of the benefit
87 for the multi-reservoir system cannot be reached by only re-designing the flood storage
88 of a single reservoir in the system. Therefore, it is necessary to analyze the mutual
89 feedback mechanism between reservoirs and their contribution to benefits from a
90 system perspective, which motivated this study. This paper is dedicated to propose a
91 new joint optimization method for design and operation of multi-reservoir system
92 considering the conditional value-at-risk ($CVaR_\alpha$).

93 $CVaR_\alpha$, a classic finance index of economic analysis, is defined as the expected
94 value of all losses above the selected probability, which can reflect the probability and
95 magnitude of damage loss simultaneously. In fact, $CVaR_\alpha$ has already been
96 commonly applied to water resources modeling (Yazdi et al., 2016), and it mainly
97 focuses on water allocation policy (Bakhtiari et al., 2020; Li et al., 2018; Shao et al.,
98 2011; Yamout et al., 2007), distribution of water rights (Hu et al., 2016; Zhang et al.,
99 2020), and risk analysis on the multi-objective water resources optimization problems
100 (Khorshidi et al., 2019; Naserizade et al., 2018; Wang et al., 2017; Zhang and Guo,
101 2018). Webby et al. (2006) optimized multi-objective problem for amenity and
102 environment flows against flood risk with the help of $CVaR_\alpha$ index. Piantadosi et al.
103 (2008) determined a policy for management of urban storm-water by combining
104 stochastic dynamic programming with $CVaR_\alpha$. Soltani et al. (2015) established an

105 objective function based on $CVaR_\alpha$ for planning agricultural water and return flow
106 allocation in river systems. Fu et al. (2018) used a conditional value-at-risk two-stage
107 stochastic programming model to plan regional water allocations. Ermoliev et al. (2019)
108 built a stochastic optimization model for risk-based reservoir management by
109 considering $CVaR_\alpha$ as a constraint. Furthermore, Zhang et al. (2018) incorporated the
110 concept of $CVaR_\alpha$ into reservoir flood damage loss evaluation and proved it is reliable
111 to take account of the $CVaR_\alpha$ value as a constraint when compared with the traditional
112 risk-based approach, which is the method basis of this study.

113 The primary purpose of this paper is to propose a new optimal method for multi-
114 reservoir systems and identify the mutual feedback mechanism between the flood
115 storage of each reservoir. The specific objective is to extend the establishment of the
116 flood damage assessment index $CVaR_\alpha$ from a single reservoir system to a multi-
117 reservoir system, and to deduce the possible feasible FSCSs for a multi-reservoir system.
118 Then, an optimization model which aims to maximize the hydropower generation
119 benefit of the multi-reservoir system is built to find the optimal reservoir flood storage
120 combination scheme.

121 The remainder of this paper is organized as follows. Section 2 describes the flood
122 damage assessment with $CVaR_\alpha$ for a single reservoir system and a multi-reservoir
123 system, and the establishment of the optimization model. A case study of Ankang-

124 Danjiangkou reservoir system is addressed in Section 3. Then, results and discussions
125 are shown in Section 4. Finally, conclusions are given in Section 5.

126 **2. Methodology**

127 The framework of the proposed joint optimization method for design and
128 operation of multi-reservoir system considering the conditional value-at-risk is shown
129 in Fig. 1, and the processes are summarized below:

130 (1) The $CVaR_\alpha$ index for the multi-reservoir system is established in the flood
131 damage assessment module, which reflects its relationship with FSCS and the
132 magnitude of design floods (Section 2.2).

133 (2) An optimal design FSCS model is proposed with the objective of maximizing
134 the hydropower generation benefits in the multi-reservoir system without increasing the
135 flood damage loss, the hydropower generation module of which is used to build the
136 relation between the objective function and FSCS (Section 2.3).

137 **[Please insert Figure 1 here]**

138 **2.1 Flood damage assessment with $CVaR_\alpha$ for a single-reservoir** 139 **system**

140 Value-at-risk (VaR_α) represents the maximum loss with a given confidence level
141 α over a specified time horizon, which is derived by using cumulative probability
142 distribution function of a random variable. $CVaR_\alpha$, a modified form of VaR_α , is
143 defined as the expected loss given that the loss exceeds VaR_α . Let $L(x, \theta)$ be a loss

144 function of a decision vector x and a stochastic vector θ . The $CVaR_\alpha$ at a given
 145 confidence level $\alpha \in [0, 1]$ can be defined as follows (Rockafellar and Uryasev, 2002):

$$\begin{aligned}
 CVaR_\alpha &= E[L(x, \theta) | \varphi(x, \theta) \geq \alpha] \\
 &= \frac{\int_{F_\alpha}^{F_{\max}} L(x, \theta) f[L(x, \theta)] dL}{1 - \alpha}
 \end{aligned} \tag{1}$$

147 where E denotes the expected value operator, F_α is the VaR_α value corresponding to
 148 a given confidence level α ($VaR_\alpha = \min[L(x, \theta) | \varphi(x, \theta) \geq \alpha]$), F_{\max} is the
 149 maximum value of loss function, $f(\cdot)$ is the probability distribution function for flood
 150 damage, $L(x, \theta)$ is a continuous or discrete loss function, and $\varphi(x, \theta)$ is the
 151 cumulative distribution function of loss. The units of variables $CVaR_\alpha$, VaR_α , F_α ,
 152 F_{\max} , $L(\cdot)$ determined by the actual application problem are the same, while the units
 153 of variables $f(\cdot)$, $\varphi(\cdot)$, α are dimensionless. It should be noted that the relationship
 154 between the confidence level α and the flood risk probability of the reservoir system
 155 R is $\alpha + R = 1$ (Detailed demonstration has been presented by Zhang et al. (2018)).

156 The reservoir flood damage assessment in this study is established by considering
 157 the reservoir downstream floodplain. $L(x, \theta)$ is a loss function for the reservoir flood
 158 storage value (m^3) (or the FLWL value (m)) x and the reservoir inflow process θ
 159 corresponding to design frequency $p(\theta)$ (%), respectively.

$$L(x, \theta) = c \cdot w_f(x, \theta) \tag{2}$$

161 where $w_f(\cdot)$ (m^3) represents the flood volume which needs to be diverted into the
 162 downstream floodplain, and c (yuan/ m^3) is the unit cost for $w_f(\cdot)$. It should be noted

163 that the unit cost of loss function is assumed as a constant, which is out of the scope of
 164 this study. The detailed description about the formulation of w_f for a single reservoir
 165 is provided in Supplement B Section by Zhang et al. (2018).

166 **2.2 Flood damage assessment with $CVaR_\alpha$ for a multi-reservoir** 167 **system**

168 The flood damage assessment for the multi-reservoir system is built as Equation
 169 3, which is extended from the single-reservoir system's flood damage assessment.

$$170 \quad CVaR_{k,\alpha} = \frac{\int_{F_{k,\alpha}}^{F_{k,\max}} L_k(x_1, x_2, \dots, x_n, \theta_k) f_k[L_k(x_1, x_2, \dots, x_n, \theta_k)] dL_k}{1 - \alpha} \quad (3)$$

171 where n is the number of upstream reservoirs corresponding to the downstream flood
 172 control point k , x_i represents the flood storage (m^3) (or the FLWL (m)) of the i th
 173 reservoir, x_1, x_2, \dots, x_n represents the flood storage combination scheme, θ_k is the
 174 multi-reservoir system's inflow process corresponding to design frequency $p(\theta_k)$ (%),
 175 $L_k(\cdot)$ is the loss function of the flood control point k , $F_{k,\alpha}$ is the $VaR_{k,\alpha}$ value
 176 corresponding to a given confidence level α , $F_{k,\max}$ is the maximum value of loss
 177 function $L_k(\cdot)$, and $f_k(\cdot)$ is the probability distribution function for flood damage
 178 corresponding to the flood control point k .

179 In application to a multi-reservoir system, the flood damage assessment index
 180 $CVaR_{k,\alpha}$ should be respectively established for sub-systems and the whole multi-
 181 reservoir system according to the downstream flood control point. Taking a two-

182 reservoir system as an example, either in series or parallel as is shown in Fig. 2, if there
 183 exists two downstream flood control points in the two-reservoir system, the conditional
 184 value-at-risk index for the sub-system and the multi-reservoir system should be
 185 constructed based on Eq. (3). The sub-system consists of the 1st reservoir and its
 186 downstream flood control point i while the multi-reservoir system contains the 1st
 187 reservoir, 2nd reservoir, and the flood control point ii .

188 **[Please insert Figure 2 here]**

189 **2.3 Optimization model for designing flood storage scheme**

190 An optimization model with the purpose of maximizing the hydropower
 191 generation benefit is established to deduce the optimal FSCS for the whole multi-
 192 reservoir system.

193 **2.3.1 Objective function**

194 Maximization of hydropower benefits for the multi-reservoir system can be
 195 described by the annual average hydropower generation during the summer flood
 196 season as follows:

$$197 \quad \max \bar{E}(x_1, x_2, \dots, x_m) = \frac{1}{T} \sum_{j=1}^T E_j(x_1, x_2, \dots, x_m) \quad (4)$$

198 where m is the number of reservoirs in the multi-reservoir system, x_i is the decision
 199 vector, representing the flood storage (m^3) of i th reservoir ($i = 1, 2, \dots, m$), $E_j(\cdot)$
 200 (kWh) represents the hydropower generation in the j^{th} year for the multi-reservoir

201 system when the reservoir flood storage combination scheme is set as x_1, x_2, \dots, x_m
 202 ($j = 1, 2, \dots, T$), $\bar{E}(\cdot)$ (kWh) represents the average annual hydropower generation for
 203 the multi-reservoir system during T years. In this study, the annual hydropower
 204 generation in the j^{th} year is calculated based on the observed data. The relationship
 205 between the average annual hydropower generation of the multi-reservoir system and
 206 the reservoir FSCS was established by conventional hydropower generation operation,
 207 which was evaluated in advance to reduce the computation time for searching for the
 208 optimal FSCS.

209 2.3.2 Constraints

210 (1) Conditional value-at-risk

$$211 \quad CVaR_{\alpha}(x_1, x_2, \dots, x_m) \leq \beta_{\alpha}(x_1^*, x_2^*, \dots, x_m^*) \quad (5)$$

212 where $\beta_{\alpha}(\cdot)$ ($c \text{ m}^3$) is the conditional value-at-risk value with the current designed
 213 reservoir FSCS $x_1^*, x_2^*, \dots, x_m^*$ corresponding to a confidence level α ; $CVaR_{\alpha}(\cdot)$ (c
 214 m^3) is the conditional value-at-risk value with the optimal variables x_1, x_2, \dots, x_m .

215 (2) Reservoir water balance equation:

$$216 \quad V_{t+1} = V_t + (I_t - Q_t) \Delta t \quad (6)$$

217 where I_t (m^3/s) and Q_t (m^3/s) are the reservoir inflow and release during time period
 218 Δt , respectively, and V_t (m^3) is the reservoir storage at time t .

219 (3) Reservoir storage limits:

$$220 \quad V_{\min} \leq V_t \leq V_{\max} \quad (7)$$

221 where V_{\min} (m^3) and V_{\max} (m^3) are the minimum and maximum allowable reservoir
222 storages during flood season.

223 (4) Release capacity limits:

$$224 \quad Q_t \leq Q_{\max}(Z_t) \quad (8)$$

225 where $Q_{\max}(Z_t)$ (m^3/s) is the reservoir maximum discharge when the reservoir water
226 level is Z_t (m) at time t .

227 (5) Initial condition:

$$228 \quad V_{1,i} = V_{\max} - x_i \quad (9)$$

229 where $V_{1,i}$ is the initial reservoir storage value of the i th reservoir.

230 The trust region reflective algorithm in MATLAB's Optimization Toolbox, which
231 returns the minimum of a nonlinear multivariate function, is chosen as the optimization
232 algorithm for the proposed optimization model because of its high computing efficiency
233 and easy use in the MATLAB programming environment.

234 3. Case study

235 3.1 Study area and data

236 The Hanjiang River has a basin area of about $159,000 \text{ km}^2$, which is the largest
237 tributary of the Yangtze River in China. Fig. 3 shows that the Ankang reservoir and
238 Danjiangkou reservoir are adjacent to each other in the main stream of the Hanjiang
239 River, and the Ankang-Danjiangkou cascade reservoir system is selected as a case study.
240 The summer flood season in the region is from late June to late August, and the

241 characteristic parameter values of the multi-reservoir system are shown in Table 1.

242 **[Please insert Figure 3 and Table 1 here]**

243 The daily streamflow data from 1954-2010 were selected as the base period dataset
244 for the Ankang Reservoir, Danjiangkou Reservoir, and Huangzhuang hydrological
245 station. The design floods were derived using the magnification method with respect to
246 several typical flood hydrographs, which is a common method used for the derivation
247 of design floods in China (Huang et al., 2020; Liu et al., 2015b; Zhang et al., 2019). In
248 this study, seven typical flood hydrographs (from 1957, 1978, 1980, 1981, 1983, 1989
249 and 2010) were selected to obtain the design floods.

250 **3.2 $CVaR_\alpha$ under the present designed FSCS condition**

251 For this two-reservoir system, the Ankang city is at the downstream flood control
252 point of the upstream Ankang reservoir, while the Huangzhuang hydrological station is
253 at the downstream flood control point of the whole Ankang-Danjiangkou reservoirs
254 system (see Fig. 2). Therefore, the Ankang-Danjiangkou Reservoirs system is divided
255 into a sub-system and a multi-reservoir system according to the two downstream flood
256 control points. Specifically, the multi-reservoir system is composed of Ankang reservoir,
257 Danjiangkou reservoir, and the Huangzhuang hydrological station, which is the focal
258 point of this study.

259 The conditional value-at-risk $\beta_{HZ,\alpha}$ corresponding to the Ankang-Danjiangkou

260 multi-reservoir's present designed FSCS during the summer flood season can be
261 derived according to Eq. (5), that is $\beta_{HZ,0.99}=6.479c$ billion yuan and
262 $\beta_{HZ,0.999}=6.481c$ billion yuan. The flood damage assessment index for the Ankang-
263 Danjiangkou multi-reservoir system during the summer flood season corresponding to
264 the different FSCS is named as $CVaR_{HZ,\alpha}$, and its upper limit value is set at the index
265 $\beta_{HZ,\alpha}$ value of the present designed FSCS.

266 **3.3 AMFS value for the reservoir in the two-reservoir system**

267 The AMFS values of the Ankang and Danjiangkou reservoirs are respectively
268 deduced through the following schemes: (i) The flood storage value of the Danjiangkou
269 reservoir is fixed at its present designed value while the Ankang reservoir's flood
270 storage changes. (ii) The flood storage value of the Ankang reservoir is fixed at its
271 present designed value while the Danjiangkou reservoir's flood storage changes. With
272 the index $\beta_{HZ,\alpha}$ corresponding to the present designed FSCS as the upper limit value
273 for the flood damage assessment index $CVaR_{HZ,\alpha}$, the AMFS values of the Ankang
274 and Danjiangkou reservoirs in the two-reservoir system can be derived to be equal to
275 0.36 billion m³ and 10.59 billion m³, respectively. Moreover, the allowable minimum
276 total flood storage value of this two-reservoir system is 10.95 billion m³.

277 4. Results and discussions

278 4.1 Feasible area for the FSCSs in the two-reservoir system

279 4.1.1 Boundary of the feasible FSCSs when fixing the two-reservoir 280 system's total flood storage (TFS)

281 The relationship between the flood damage assessment index and flood storage
282 values of the two reservoirs is shown in Fig. 4, $CVaR_\alpha$ values for a given confidence
283 level $\alpha = 0.99$ first decrease significantly as the flood storage of the Danjiangkou
284 reservoir (or Ankang reservoir) increases and then stabilize at a certain value when the
285 flood storage value of the Ankang reservoir (or Danjiangkou reservoir) is fixed.
286 However, the loss function of the flood damage for the two-reservoir system in this
287 study is the expression of three variables, i.e., the Ankang reservoir's flood storage, the
288 Danjiangkou reservoir's flood storage, and the inflow magnitude, thus, it is difficult to
289 directly judge the relationship between the loss function L_{HZ} (or the $CVaR_{HZ,\alpha}$ value)
290 and the FSCS of the two reservoirs in the system because of the high dimension.

291 **[Please insert Figure 4 here]**

292 In order to clarify the influence of different FSCSs on the flood damage assessment
293 index $CVaR_\alpha$, Scenario 1 is established as follows: The Ankang-Danjiangkou
294 Reservoirs system's TFS during the summer flood season is fixed at a constant value,
295 and then the FSCSs of the two reservoirs change. Considering that present designed
296 flood storage values of the Ankang and Danjiangkou reservoirs are 0.36 billion m^3 and

297 11.00 billion m³ in the summer flood season, respectively, TFS value of this two-
298 reservoir system is assumed to be fixed at 11.36 billion m³. Then, the flood storage
299 value of the Ankang reservoir changes from 0.01 billion m³ to 1.41 billion m³, and the
300 Danjiangkou reservoir's flood storage is adjusted with the change of the Ankang
301 reservoir's flood storage.

302 **[Please insert Figure 5 here]**

303 Fig. 5(a) and Table 2 show the results of Scenario 1 when FSCSs for the two
304 reservoirs change, which are numbered from 1 to 29 in sequence. The flood damage
305 assessment index $CVaR_{HZ,\alpha}$ of this multi-reservoir system during the summer flood
306 season presents a decreasing trend in schemes 1 to 8, keeps at a constant value in
307 schemes 8 to 16, and finally increases in schemes 16 to 29. Therefore, one point can be
308 drawn from the analysis results in Scenario 1, that is, the $CVaR_{HZ,\alpha}$ value of the multi-
309 reservoir system varies if FSCSs of the Ankang and Danjiangkou reservoirs change
310 even though the TFS value is fixed at a constant value. In addition, FSCSs from
311 schemes 8 to 16 are the feasible schemes in the summer flood season, which are called
312 feasible intervals of FSCSs, with conditional value-at-risk $\beta_{HZ,\alpha}$ values under the
313 present designed FSCS (see Section 3.2) as the upper limit values.

314 In order to explore the boundary condition of FSCS's feasible intervals for multi-
315 reservoir systems, several FSCSs are added. The left boundary of the feasible interval
316 for FSCSs is obtained where the Ankang reservoir's flood storage value is equal to 0.36

317 billion m³ (Fig. 5(b)). In Fig. 5(c), the right boundary of the feasible interval for FSCSs
318 is acquired where the Danjiangkou reservoir's flood storage value is 10.59 billion m³.
319 It should be emphasized that the terms "left" and "right" here correspond to the situation
320 for convenience of expression, of which the flood storage value of Ankang reservoir
321 during the summer flood season changes from 0.01 billion m³ to 1.41 billion m³ and
322 the flood storage value of Danjiangkou reservoir changes accordingly to keep TFS at a
323 constant value.

324 If TFS of this two-reservoir system ranges from 10.95 billion m³ (the allowable
325 minimum TFS derived in Section 3.3) to 11.36 billion m³ (the present designed TFS
326 given in Table 1), the feasible FSCSs can be represented as a triangle area (Fig. 6), and
327 the red line corresponds to the feasible interval of FSCSs in Scenario 1 (i.e., scheme 8
328 to 16 in Fig. 5). It should be noted that V_{AK} and V_{DK} respectively represent Ankang
329 and Danjiangkou reservoirs' flood storage values in Figure 6.

330 **[Please insert Figure 6 here]**

331 **4.1.2 Discussion on the shape of feasible FSCSs area**

332 On the basis of Scenario 1, the flood damage assessment index $CVaR_\alpha$ of the
333 two-reservoir system corresponding to that the TFS in the summer flood season
334 successively fixed in the range of 10.95 billion m³ to 15.13 billion m³ is estimated, the
335 result of which is shown in Figure 7(a). If the TFS of multi-reservoir system is smaller
336 than and equal to 12.024 billion m³, the shape for feasible FSCSs area is a triangle; if

337 the TFS of this two-reservoir system is larger than 12.024 billion m³, the shape of
 338 feasible FSCSs area turns into a right-angled trapezoid because of the Ankang
 339 reservoir's flood storage value reaches its maximum. In addition, V_{AK}^D and V_{DJK}^D are
 340 the Ankang and Danjiangkou reservoirs' AMFS values, respectively, while V_{AK}^U and
 341 V_{DJK}^U are the Ankang and Danjiangkou reservoirs' maximum flood storage values
 342 which are determined by the characteristic of the reservoir itself.

343 Only two scenario results (shown in Fig. 7(b) and Fig. 7(c)) are selected for further
 344 analysis because of the obvious regularity of the all scenarios and the inconvenience of
 345 displaying them all. Fig. 7(b) shows $CVaR_{HZ,\alpha}$ values when the multi-reservoir
 346 system's TFS is fixed at 11.67 billion m³ (i.e., the gray line in Fig. 7(a)), and
 347 furthermore the left and right boundaries of the feasible interval of FSCSs are obtained
 348 at AMFS values of the Ankang and Danjiangkou reservoirs, respectively. The value of
 349 $CVaR_{HZ,\alpha}$ first decreases as the Ankang reservoir's flood storage increases, and then
 350 goes through an interval to stabilize, which is called the feasible interval of the FSCSs.
 351 However, the $CVaR_{HZ,\alpha}$ value increases significantly when the flood storage of
 352 Ankang reservoir is larger (that is, the corresponding Danjiangkou reservoir's flood
 353 storage is smaller). The above results show the same regular pattern as Fig. 5(a). Fig.
 354 7(c) presents $CVaR_{HZ,\alpha}$ values when the TFS is fixed at 12.17 billion m³ (i.e., the
 355 green line in Fig. 7(a)), and the left boundary of the feasible interval of FSCSs is the
 356 Ankang reservoir's AMFS. However, the right boundary of feasible FSCSs interval

357 does not exist because the flood storage value of Danjiangkou reservoir is always larger
358 than its AMFS value. It should be noted that the result given in Fig. 7(c) is a special
359 case because of the big difference in the flood capacity levels of two reservoirs, which
360 is not inconsistent with the conclusion in Section 4.1.1.

361 **[Please insert Figure 7 here]**

362 Comparison results between the shape of feasible FSCSs area derived by the
363 $CVaR_\alpha$ index (see the area filled with green stippled lines in Fig. 8(d)) and the
364 traditional risk-based method (see the area filled with the blue triangle in Fig. 8(d)) are
365 shown in Fig. 8, and the detailed certification process is given in Appendix A. Feasible
366 FLWLs of this study is inferred from the design level while that of Chen et al. (2012)
367 is inferred by considering the streamflow forecast information at the real-time operating
368 level. Furthermore, previous studies, including Chen et al. (2012), about the feasible
369 FLWLs paid more attention to the upper limit of the reservoir water level during the
370 flood season by making full use of the forecast information, and the static FLWL was
371 conventionally used as the lower limit in order not to sacrifice the power generation
372 benefit. However, the lower limit value of feasible FLWL combination deduced by the
373 flood damage assessment index $CVaR_\alpha$ is not as small as possible because of the flood
374 capacity restraints for the whole multi-reservoir system and each sub-system.

375 **[Please insert Figure 8 here]**

376 **4.1.3 Discussion on the sensitivity of $CVaR_\alpha$ to the flood storage of**
377 **each reservoir**

378 Scenario 2 aims to analyze the influence of each reservoir's flood storage value on
379 the $CVaR_\alpha$ value of the multi-reservoir system as follows: The Ankang (Danjiangkou)
380 reservoir's flood storage value is fixed as a constant value, while the flood storage value
381 of Danjiangkou (Ankang) reservoir changes, and vice versa. Figure 9 shows the results
382 of Scenario 2, and the change in $CVaR_{HZ,\alpha}$ value caused by the unit flood storage
383 change of Danjiangkou reservoir is greater when compared with that of the Ankang
384 reservoir. Therefore, the $CVaR_{HZ,\alpha}$ value is more sensitive to changes in the flood
385 storage of Danjiangkou reservoir than that of Ankang reservoir because of the
386 difference of reservoir flood storage capacity and upstream and downstream positional
387 relationship of the two reservoirs. Furthermore, the discussion on a five-reservoir
388 system is given in Appendix B, and the conclusion can be drawn as following: a) if the
389 positional relationship between the two reservoirs is parallel, the greater the reservoir
390 flood control capacity, the lower the sensitivity of $CVaR_\alpha$ to the amplitude of the flood
391 storage value; b) if the two reservoirs are in series position, the sensitivity of $CVaR_\alpha$
392 to the amplitude of flood storage value for the downstream reservoir is higher than that
393 for the upstream reservoir.

394 **[Please insert Figure 9 here]**

395 **4.2 Trade-offs between flood damage and hydropower benefit by**
396 **considering the $CVaR_\alpha$ index**

397 The flood control benefits provided by the feasible FSCSs of Ankang-
398 Danjiangkou Reservoirs system are the same from the perspective of the flood damage
399 assessment $CVaR_\alpha$ index. However, the trade-offs between activities of flood control
400 and hydropower generation need to be further explored (Rheinheimer et al., 2016; Wang
401 et al., 2021), and then an optimization model (Section 2.3) was used to search for the
402 optimal FSCS from the feasible FSCSs.

403 **[Please insert Figure 10 here]**

404 The TFS of the two-reservoir system is fixed at its present designed value (i.e.,
405 11.36 billion m^3) in Figure 10, the red points represent the hydropower generation
406 benefit (i.e., plus character) and flood damage assessment index $CVaR_{HZ,\alpha}$ values (i.e.,
407 triangular and square characters) corresponding to the optimal FSCS. Further
408 discussions are conducted from the following aspects:

409 (1) The relationship between the hydropower generation benefit and the flood
410 damage assessment index $CVaR_\alpha$ is not monotonic. Thus, the feasible FSCSs of the
411 multi-reservoir system taking the constraint of $CVaR_\alpha$ value into consideration should
412 be used as a prerequisite for seeking the optimal solution where the maximum
413 hydropower generation benefit is obtained.

414 (2) Fig. 10 reveals the larger the flood storage value of Ankang reservoir, the lesser

415 the hydropower generation benefit of two-reservoir system. In other words, if the TFS
416 of the two-reservoir system is fixed, the flood storage is suggested allocated to the
417 Danjiangkou reservoir (the downstream reservoir in this two-reservoir system) with the
418 purpose of maximizing the hydropower generation benefit.

419 **[Please insert Figure 11 here]**

420 Optimal results when the Ankang-Danjiangkou Reservoirs system's TFS in the
421 summer flood season is successively fixed in the range of 10.95 billion m³ to 13.95
422 billion m³ are shown in Figure 11. It should be noted that all the FSCSs shown in Fig.
423 11 satisfy the constraint of the flood assessment $CVaR_\alpha$ index. Several points can be
424 drawn as follows:

425 (1) The maximization value of the hydropower generation benefit was achieved
426 where both the Ankang and Danjiangkou reservoirs' flood storage values are equal to
427 their AMFS values (the red asterisk point shown in Fig. 11): The Ankang reservoir's
428 flood storage value is 0.36 billion m³ while the Danjiangkou reservoir's flood storage
429 value is 10.59 billion m³.

430 (2) The optimal results in Fig. 11 reveal the conflict relationship between the
431 hydropower generation benefit and the TFS, i.e., the larger the TFS, the lesser the
432 hydropower generation benefit of the two-reservoir system. Moreover, there is also a
433 monotonous decreasing relationship between the hydropower generation benefit and
434 each single reservoir's flood storage value in the Ankang-Danjiangkou Reservoirs

435 system.

436 **5. Conclusions**

437 This paper proposed a new joint optimization method for design and operation of
438 multi-reservoir system considering the index $CVaR_\alpha$, and focused on analyzing the
439 mutual feedback mechanism between the flood storage of each reservoir in the systems.

440 The main findings are made as follows:

441 (1) The $CVaR_\alpha$ values of the multi-reservoir system vary if FSCSs of the
442 Ankang and Danjiangkou reservoirs are different even though the TFS is set to the same
443 constant value. The feasible area of FSCSs derived by considering the $CVaR_\alpha$ index
444 can be described as a triangle, and the boundary of this feasible interval is determined
445 by the AMFS value of reservoirs in the mixed multi-reservoir system.

446 (2) The contribution degree of each reservoir to flood control benefits can be
447 summarized as following: a) if the reservoirs are in parallel positions, the greater the
448 reservoir flood control capacity, the lower the sensitivity of $CVaR_\alpha$ to the amplitude
449 of the flood storage value; b) if the reservoirs are in series position, the sensitivity of
450 $CVaR_\alpha$ to the amplitude of flood storage value for the downstream reservoir is higher
451 than that for the upstream reservoir.

452 (3) The relationship between the hydropower generation benefit and the flood
453 damage assessment index $CVaR_\alpha$ is not monotonic. The joint optimal design of multi-
454 reservoir system FSCS can be deduced by establishing an optimal model with the
455 purpose of maximizing the hydropower generation benefit for the whole multi-reservoir

456 system. The global optimal solution of the hydropower generation benefit was achieved
457 when all reservoirs' flood storage values were respectively equal to their AMFS.

458 It's worth noting that the index $CVaR_\alpha$ can be applied in multi-reservoir system
459 (more than two reservoirs) with following steps: (i) System division is conducted
460 according to the protection object of downstream flood control point (refer to Section
461 2.2). (ii) Flood damage assessment indexes $CVaR_\alpha$ for the sub-system and the whole
462 multi-reservoir system are respectively established to deduce the AMFS of each
463 reservoir and the FSCSs for the multi-reservoir system (refer to Section 4.1.1). In
464 addition, the relationship between any two reservoirs in the system can be derived by
465 dividing the multi-reservoir system into several two-reservoir sub-systems. The
466 establishment of the flood damage assessment index by taking the concept of $CVaR_\alpha$
467 into consideration can be more accurate if the relevant actual socioeconomic data is
468 available. For example, the unit cost c of loss function is assumed constant, which
469 can be determined or further researched when the economic assessment of flood control
470 losses for the specific study area is provided. The $CVaR_\alpha$ value would be applied in
471 the multi-objective optimization operation fields by coupling the benefit targets (such
472 as hydropower generation benefit, water supply benefit) since it can reflect the possible
473 flood damage loss. Moreover, the feasible interval of the flood storage for a multi-
474 reservoir system derived in this paper can help understand the research on the dynamic
475 control of the FLWLs in multi-reservoir systems.

476 **Author statement**

477 **Zhang Xiaoqi:** Conceptualization, Methodology, Software Writing- Original
478 Draft **Liu Pan:** Conceptualization, Supervision, Writing- Review & Editing **Feng**
479 **Maoyuan:** Methodology, Validation, Writing- Review & Editing **Xu Chong-Yu:**
480 Supervision, Writing- Review & Editing **Cheng Lei:** Validation, Writing- Review &
481 Editing **Gong Yu:** Data Curation, Writing- Review & Editing

482 **Declaration of Competing Interest**

483 The authors declare that they have no known competing financial interests or
484 personal relationships that could have appeared to influence the work reported in this
485 paper.

486 **Acknowledgments**

487 This study was supported by National Natural Science Foundation of China (Grant
488 No. 521090003, 41890822, 51861125102), and Joint Funds of the National Natural
489 Science Foundation of China (Grant No. U1865201).

490 **Appendix A: Derivation for the shape of the feasible FSCSs area by**
491 **the $CVaR_\alpha$ index and the traditional risk-based method**

492 The feasible FSCSs of the two-reservoir system obtained through the flood
493 damage assessment index $CVaR_\alpha$ are shown as a triangle area (see Figure 7(a)), which
494 is simplified into a schematic diagram (see Figure 8(a)) for the convenience of
495 explanation. The feasible FSCSs area is determined by the following variables: (i) the
496 allowable maximum flood storage of reservoir A, V_A^U ; (ii) the allowable minimum

497 flood storage (AMFS) of reservoir A, V_A^D , which corresponds to the static control of
 498 FLWL for reservoir A; (iii) the allowable maximum flood storage of reservoir B, V_B^U ;
 499 (iv) the AMFS of reservoir B, V_B^D , which corresponds to the static control of FLWL
 500 for reservoir B. In addition, the terms V_A^U and V_B^U are both assumed to not exceed
 501 their maximum storage capacity constraints. The coordinates of the points f and g of
 502 the red line in Fig. 8(a) are respectively (V_B^D, V_A^U) and (V_B^U, V_A^D) , which satisfy the
 503 curve equation as follows:

$$504 \quad V_A + V_B \cdot K = M \quad (A1)$$

505 where V_A and V_B are the reservoir flood storage values of reservoir A and B,
 506 respectively, and the term (V_B, V_A) is the point on the curve Equation A1. Parameter
 507 K is the slope of the linear function, and parameter M is the intercept from the
 508 perspective of mathematical theory. Then, parameters $K = (V_A^U - V_A^D) / (V_B^U - V_B^D) > 0$
 509 and $M = (V_A^U \cdot V_A^D - V_B^U \cdot V_B^D) / (V_B^U - V_B^D)$ can be deduced by solving the equation A2.

$$510 \quad \begin{cases} V_A^U + V_B^D \cdot K = M \\ V_A^D + V_B^U \cdot K = M \end{cases} \quad (A2)$$

511 In Figure 8(b), the feasible FLWL combination schemes of the two-reservoir
 512 system derived by Chen et al. (2012) is described as a Fan-shaped area, which is
 513 deduced through the traditional risk-based approach. The feasible FLWLs area is
 514 determined by the following variables: (i) the allowable maximum FLWL of reservoir
 515 A, Z_A^* , which is determined by the dynamic control of FLWL; (ii) the allowable
 516 minimum FLWL of reservoir A, Z_A^U , which is equal to the static control of FLWL; (iii)

517 the allowable maximum FLWL of reservoir B, Z_B^* , which is determined by the
518 dynamic control of FLWL; (iv) the allowable minimum FLWL of reservoir B, Z_B^U . In
519 order to better compare the area size acquired by these two different methods, the
520 feasible FSCSs of the two-reservoir system in Figure 8(a) should be converted to a
521 feasible FLWLs which is unified with the characterization variable with Figure 8(b). It
522 should be noted that the relationship between the reservoir water level Z_j and the
523 flood storage V_j is assumed as a power function form (Mohammadzadeh-Habili and
524 Heidarpour, 2010; Zhang et al., 2019b) and is shown in Equation A3.

$$525 \quad Z_j = a_j S_j^{b_j} = a_j (V_{j,n} - V_j)^{b_j} \quad (\text{A3})$$

526 where S_j is the water stored in the reservoir, $V_{j,n}$ is the reservoir storage
527 corresponding to its normal pool level, a_j and b_j are parameters of the power
528 function, $a_j > 1$ and $0 < b_j < 1$, $j = A \text{ or } B$.

529 The variables Z_A^D and Z_A^U are respectively the reservoir water levels
530 corresponding to the reservoir flood storage values V_A^U and V_A^D . In Fig. 8(c), and the
531 key point is to clarify the position of the envelope of the feasible FLWLs area. Based
532 on Equations A1 and A3, the relationship between variables and can be described as Eq.
533 (A4).

$$534 \quad Z_A = a_A \cdot \left[H - c_B \cdot (Z_A)^{d_B} \right]^{b_A} > 0 \quad (\text{A4})$$

535 where $a_A > 1$, $0 < b_A < 1$, $c_B = K \cdot \left(\frac{1}{a_B} \right)^{\frac{1}{b_B}} > 0$, $d_B = \frac{1}{b_B} > 1$, and

$$536 \quad H = V_{A,n} + V_{B,n} - M > 0.$$

537 The derivation results for signs of $\partial Z_A / \partial Z_B$ and $\partial^2 Z_A / \partial (Z_B)^2$ are shown in
 538 Eqs. (A5)-(A6), indicating that ∂Z_A decreases when ∂Z_B increases and that ∂Z_B
 539 has a diminishing marginal contribution to ∂Z_A . Therefore, the type of envelope in Fig.
 540 8(c) should be the type I (green dotted line).

$$541 \quad \frac{\partial Z_A}{\partial Z_B} = -a_A b_A c_B d_B (Z_B)^{d_B-1} \cdot [H - c_B \cdot (Z_B)^{d_B}]^{b_A-1} < 0 \quad (A5)$$

$$542 \quad \begin{aligned} \frac{\partial^2 Z_A}{\partial Z_B^2} &= -a_A b_A c_B d_B (d_B - 1) (Z_B)^{d_B-2} \cdot [H - c_B \cdot (Z_B)^{d_B}]^{b_A-1} \\ &+ a_A b_A c_B d_B (Z_B)^{d_B-1} \cdot (b_A - 1) \cdot [H - c_B \cdot (Z_B)^{d_B}]^{b_A-2} \cdot c_B \cdot d_B (Z_B)^{d_B-1} \quad (A6) \\ &= -\frac{a_A b_A c_B d_B (Z_B)^{d_B-2}}{[H - c_B \cdot (Z_B)^{d_B}]^{1-b_A}} \cdot \left\{ (d_B - 1) + \frac{(1-b_A) c_B d_B (Z_B)^{d_B}}{H - c_B \cdot (Z_B)^{d_B}} \right\} < 0 \end{aligned}$$

543 The comparison results between the feasible FLWLs obtained by the index
 544 $CVaR_\alpha$ and the traditional flood risk probability, respectively are shown in Fig. 8(d).

545 **Appendix B: Discussion on the sensitive of $CVaR_\alpha$ to the flood storage** 546 **of each reservoir in a five-reservoir system**

547 The flood damage assessment index $CVaR_\alpha$ for the multi-reservoir system
 548 proposed in Section 2.2 is applied in a five-reservoir system in order to identify the
 549 sensitive factor for the relationship between the $CVaR_\alpha$ value and the reservoir flood
 550 storage. A five-reservoir system, which includes the Ankang, Pankou, Danjiangkou,
 551 Sanliping and Yahekou reservoirs, is extended from the two-reservoir system in Section
 552 4.1.3, and the location relationship among these five reservoirs is shown in Fig. B1.

553 The results of relationship between the flood damage assessment index $CVaR_\alpha$

554 value and Pankou/Sanliping/Yahekou reservoirs's flood storage value are shown in Fig.
555 B2 (Results for Ankang/Danjiangkou reservoirs are shown in Fig. 9). The flood control
556 capacity of the five reservoirs in descending order are: Danjiangkou, Pankou, Ankang,
557 Yahekou, Sanliping reservoirs. As shown in Fig. B2, the sensitivity of $CVaR_\alpha$ to the
558 amplitude of the flood storage value for the five reservoirs in descending order are:
559 Sanliping, Yahekou, Danjiangkou, Ankang, Pankou reservoirs. Several points can be
560 concluded as follows:

561 a) When the reservoirs are in parallel relationship, the greater the reservoir flood
562 control capacity, the lower the sensitivity of $CVaR_\alpha$ to the amplitude of the flood
563 storage value. Facing the common downstream flood control point, parallel reservoirs
564 affect the flood control effect by separately undertaking the flood regulation of the river
565 channels in their respective locations. Therefore, the reservoir with the smaller flood
566 control capacity should be paid more attention in the case of encountering the same
567 design frequency of inflow. Furthermore, it is recommended to allocate the new unit
568 storage to the reservoir with smaller flood control capacity among the parallel reservoirs
569 when the system's total flood storage (TFS) needs to increase, so as to greatly reduce
570 the potential flood damage (i.e., the $CVaR_\alpha$ value). Conversely, if the TFS decreases,
571 it is recommended to adjust the reservoir with larger flood control capacity among the
572 parallel reservoirs, which can minimize the increase in the multi-system's potential
573 flood control losses.

574 b) If the reservoirs are in series position, the sensitivity of $CVaR_\alpha$ to the
575 amplitude of flood storage value for the downstream reservoir is higher than that for
576 the upstream reservoir. For series reservoirs, the downstream reservoir is to regulate
577 both the release from the upstream reservoir and the interval inflow. Therefore,
578 compared with the upstream reservoir, the downstream reservoir has a greater sphere
579 of influence in regulation of flood control points in the multi-reservoir system. If the
580 TFS increases, the added unit storage is advised to the downstream reservoir, which can
581 greatly lessen the potential flood damage. On the contrary, if the TFS decreases, it is
582 recommended to reduce the upstream reservoir's flood storage with the purpose of
583 decreasing the increment of the $CVaR_\alpha$ value.

584 **References**

- 585 Bakhtiari, P.H., Nikoo, M.R., Izady, A., Talebbeydokhti, N., 2020. A coupled agent-based risk-based
586 optimization model for integrated urban water management. *Sustainable Cities and Society*, 53:
587 101922. DOI:10.1016/j.scs.2019.101922
- 588 Chen, J.H., Guo, S.L., Li, Y., Liu, P., Zhou, Y.L., 2012. Joint Operation and Dynamic Control of Flood
589 Limiting Water Levels for Cascade Reservoirs. *Water Resources Management*, 27(3): 749-763.
590 DOI:10.1007/s11269-012-0213-z
- 591 Cheng, Q., Ming, B., Liu, P., Huang, K.D., Gong, Y., Li, X., Zheng, Y., 2021. Solving hydro unit
592 commitment problems with multiple hydraulic heads based on a two-layer nested optimization
593 method. *Renewable Energy*, 172: 317-326.
- 594 Dogan, M.S., Lund, J.R., Medellin-Azuara, J., 2021. Hybrid Linear and Nonlinear Programming Model
595 for Hydropower Reservoir Optimization. *Journal of Water Resources Planning and
596 Management*, 147(3): 06021001. DOI:10.1061/(ASCE)WR.1943-5452.0001353
- 597 Ermoliev, Y. Ermolieva, T., Kahil, T., Obersteiner, M., Gorbachuk, V., Knopov, P., 2019. Stochastic
598 Optimization Models for Risk-Based Reservoir Management. *Cybernetics and Systems
599 Analysis*, 55(1): 55-64. DOI:10.1007/s10559-019-00112-z
- 600 Fu, Q. Li, L.Q., Li, M., Li, T.X., Liu, D., Hou, R.J., Zhou, Z.Q., 2018. An interval parameter conditional
601 value-at-risk two-stage stochastic programming model for sustainable regional water allocation
602 under different representative concentration pathways scenarios. *Journal of Hydrology*, 564:
603 115-124. DOI:10.1016/j.jhydrol.2018.07.008

604 Gong, Y. Liu, P., Cheng, L., Chen, G.Y., Zhou, Y.L., Zhang, X.Q., Xu, W.F., 2020. Determining dynamic
605 water level control boundaries for a multi-reservoir system during flood seasons with
606 considering channel storage. *Journal of Flood Risk Management*, 13(1): e12586.
607 DOI:10.1111/jfr3.12586

608 He, S.K., Guo, S.L., Chen, K.B., Deng, L.L., Liao, Z., Xiong, F., Yin, J.B., 2019. Optimal impoundment
609 operation for cascade reservoirs coupling parallel dynamic programming with importance
610 sampling and successive approximation. *Advances in Water Resources*, 131: 103375.
611 DOI:10.1016/j.advwatres.2019.07.005

612 Hu, Z.N., Wei, C.T., Yao, L.M., Li, L., Li, C.Z., 2016. A multi-objective optimization model with
613 conditional value-at-risk constraints for water allocation equality. *Journal of Hydrology*, 542:
614 330-342. DOI:10.1016/j.jhydrol.2016.09.012

615 Huang, Z. Zhao, T.T.G., Liu, Y., Zhang, Y.Y., Jiang, T., Lin, K.R., Chen, X.H., 2020. Differing roles of
616 base and fast flow in ensemble seasonal streamflow forecasting: An experimental investigation.
617 *Journal of Hydrology*, 591: 125272. DOI:10.1016/j.jhydrol.2020.125272

618 Hui, R., Lund, J.R., 2015. Flood Storage Allocation Rules for Parallel Reservoirs. *Journal of Water
619 Resources Planning and Management*, 141(5): 04014075. DOI:10.1061/(ASCE)WR.1943-
620 5452.0000469

621 Jiang, Z.Q., Sun, P., Ji, C.M., Zhou, J.Z., 2015. Credibility theory based dynamic control bound
622 optimization for reservoir flood limited water level. *Journal of Hydrology*, 529: 928-939.
623 DOI:10.1016/j.jhydrol.2015.09.012

624 Khorshidi, M.S., Nikoo, M.R., Sadegh, M., Nematollahi, B., 2019. A Multi-Objective Risk-Based Game
625 Theoretic Approach to Reservoir Operation Policy in Potential Future Drought Condition.
626 *Water Resources Management*, 33(6): 1999-2014. DOI:10.1007/s11269-019-02223-w

627 Li, Q.Q., Li, Y.P., Huang, G.H., Wang, C.X., 2018. Risk aversion based interval stochastic programming
628 approach for agricultural water management under uncertainty. *Stochastic Environmental
629 Research and Risk Assessment*, 32(3): 715-732. DOI:10.1007/s00477-017-1490-0

630 Liu, D.D., Li, X., Guo, S.L., Rosbjerg, D., Chen, H., 2015a. Using a Bayesian Probabilistic Forecasting
631 Model to Analyze the Uncertainty in Real-Time Dynamic Control of the Flood Limiting Water
632 Level for Reservoir Operation. *Journal of Hydrologic Engineering*, 20(2): 04014036.
633 DOI:10.1061/(ASCE)HE.1943-5584.0000979

634 Liu, P., Li, L.P., Guo, S. L., Xiong, L.H., Zhang, W., Zhang, J.W., Xu, C-Y., 2015b. Optimal design of
635 seasonal flood limited water levels and its application for the Three Gorges Reservoir. *Journal
636 of Hydrology*, 527: 1045-1053. DOI:10.1016/j.jhydrol.2015.05.055

637 Ming, B., Liu, P., Cheng, L., 2021. An integrated framework for optimizing large hydro–photovoltaic
638 hybrid energy systems: Capacity planning and operations management. *Journal of Cleaner
639 Production*, 306: 127253.

640 Naserizade, S.S., Nikoo, M.R., Montaseri, H., 2018. A risk-based multi-objective model for optimal
641 placement of sensors in water distribution system. *Journal of Hydrology*, 557: 147-159.
642 DOI:10.1016/j.jhydrol.2017.12.028

643 Ouyang, S., Zhou, J., Li, C., Liao, X., Wang, H., 2015. Optimal Design for Flood Limit Water Level of
644 Cascade Reservoirs. *Water Resources Management*, 29(2): 445-457. DOI:10.1007/s11269-014-

645 0879-5

646 Piantadosi, J., Metcalfe, A.V., Howlett, P.G., 2008. Stochastic dynamic programming (SDP) with a
647 conditional value-at-risk (CVaR) criterion for management of storm-water. *Journal of*
648 *Hydrology*, 348(3-4): 320-329. DOI:10.1016/j.jhydrol.2007.10.007

649 Rheinheimer, D.E., Bales, R.C., Oroza, C.A., Lund, J.R., Viers, J.H., 2016. Valuing year-to-go hydrologic
650 forecast improvements for a peaking hydropower system in the Sierra Nevada. *Water Resources*
651 *Research*, 52(5): 3815-3828. DOI:10.1002/2015WR018295

652 Rockafellar, R.T., Uryasev, S., 2002. Conditional value-at-risk for general loss distributions. *Journal of*
653 *Banking & Finance*, 26(7): 1443-1471.

654 Shao, L.G., Qin, X.S., Xu, Y., 2011. A conditional value-at-risk based inexact water allocation model.
655 *Water Resources Management*, 25(9): 2125-2145. DOI:10.1007/s11269-011-9799-9

656 Soltani, M., Kerachian, R., Nikoo, M.R., Noory, H., 2015. A conditional value at risk-based model for
657 planning agricultural water and return flow allocation in river systems. *Water Resources*
658 *Management*, 30(1): 427-443. DOI:10.1007/s11269-015-1170-0

659 Tan, Q.F., Wang, X., Liu, P., Lei, X.H., Cai, S.Y., Wang, H., Ji, Y., 2017. The Dynamic Control Bound of
660 Flood Limited Water Level Considering Capacity Compensation Regulation and Flood Spatial
661 Pattern Uncertainty. *Water Resources Management*, 31(1): 143-158. DOI:10.1007/s11269-016-
662 1515-3

663 Wang, J., Zhao, T., Zhao, J., Wang, H., Lei, X., 2021. Improving real-time reservoir operation during
664 flood season by making the most of streamflow forecasts. *Journal of Hydrology*, 595: 126017.
665 DOI:10.1016/j.jhydrol.2021.126017

666 Wang, Y.Y., Huang, G.H., Wang, S., 2017. CVaR-based factorial stochastic optimization of water
667 resources systems with correlated uncertainties. *Stochastic Environmental Research and Risk*
668 *Assessment*, 31(6): 1543-1553. DOI:10.1007/s00477-016-1276-9

669 Webby, R.B., Boland, J., Howlett, P., Metcalfe, A.V., Sritharan, T., 2006. Conditional value-at-risk for
670 water management in Lake Burley Griffin. *ANZIAM Journal*, 47: C116-C136.

671 Yamout, G.M., Hatfield, K., Romeijn, H.E., 2007. Comparison of new conditional value-at-risk-based
672 management models for optimal allocation of uncertain water supplies. *Water Resources*
673 *Research*, 43(7): W07430. DOI:10.1029/2006wr005210

674 Yazdi, J., Torshizi, A.D., Zahraie, B., 2016. Risk based optimal design of detention dams considering
675 uncertain inflows. *Stochastic Environmental Research and Risk Assessment*, 30(5): 1457-1471.
676 DOI:10.1007/s00477-015-1171-9

677 Yeh, W.-G., William, 1985. Reservoir Management and Operations Models: A State-of-the-Art Review.
678 *Water Resources Research*, 21(12): 1797-1818.

679 Yun, R., Singh, V.P., 2008. Multiple duration limited water level and dynamic limited water level for
680 flood control, with implications on water supply. *Journal of Hydrology*, 354(1): 160-170.
681 DOI:10.1016/j.jhydrol.2008.03.003

682 Zhang, C., Guo, P., 2018. An inexact CVaR two-stage mixed-integer linear programming approach for
683 agricultural water management under uncertainty considering ecological water requirement.
684 *Ecological Indicators*, 92: 342-353. DOI:10.1016/j.ecolind.2017.02.018

685 Zhang, L., Zhang, X., Wu, F., Pang, Q., 2020. Basin Initial Water Rights Allocation under Multiple

686 Uncertainties: a Trade-off Analysis. *Water Resources Management*, 34(3): 955-988.
687 DOI:10.1007/s11269-019-02453-y
688 Zhang, X., Liu, P., Xu, C-Y., Gong, Y., Cheng, L., He, S.K., 2019. Real-time reservoir flood control
689 operation for cascade reservoirs using a two-stage flood risk analysis method. *Journal of*
690 *Hydrology*, 577. DOI:10.1016/j.jhydrol.2019.123954
691 Zhang, X., Liu, P., Xu, C-Y., Ming, B., Xie, A.L., Feng, M.Y., 2018. Conditional Value-at-Risk for
692 Nonstationary Streamflow and Its Application for Derivation of the Adaptive Reservoir Flood
693 Limited Water Level. *Journal of Water Resources Planning and Management*, 144(3): 04018005.
694 DOI:10.1061/(ASCE)WR.1943-5452.0000906
695 Zhou, Y., Guo, S., Chang, F-J., Liu, P., Chen, A.B., 2018. Methodology that improves water utilization
696 and hydropower generation without increasing flood risk in mega cascade reservoirs. *Energy*,
697 143: 785-796. DOI:10.1016/j.energy.2017.11.035
698 Zhou, Y., Guo, S., Liu, P., Xu, C., 2014. Joint operation and dynamic control of flood limiting water
699 levels for mixed cascade reservoir systems. *Journal of Hydrology*, 519: 248-257.
700 DOI:10.1016/j.jhydrol.2014.07.029
701

702 **Tables**703 **Table 1.** Characteristic parameter values for the Ankang-Danjiangkou reservoirs.

Reservoir	Parameter	Unit	Value
Ankang reservoir	Flood storage in the summer flood season	billion m ³	0.36
	FLWL during the summer flood season	m	325.0
	Normal pool level	m	330.0
	Dead water level	m	305.0
Danjiangkou reservoir	Flood storage in the summer flood season	billion m ³	11.0
	FLWL during the summer flood season	m	160.0
	Normal pool level	m	170.0
	Dead water level	m	155.0

704

705 **Table 2.** Calculation results of Scenario 1: the total flood storage of the Ankang-Danjiangkou Reservoirs system during the summer flood season is fixed at a constant
706 value, and then the FSCSs of the two reservoirs changes.

Scheme number	Ankang reservoir's flood storage (10^8 m^3)	Danjiangkou reservoir's flood storage (10^8 m^3)	Total flood storage (10^8 m^3)	$CVaR_{HZ,\alpha}(c \ 10^8 \text{ m}^3)$		Scheme number	Ankang reservoir's flood storage (10^8 m^3)	Danjiangkou reservoir's flood storage (10^8 m^3)	Total flood storage (10^8 m^3)	$CVaR_{HZ,\alpha}(c \ 10^8 \text{ m}^3)$	
				$\alpha=0.999$	$\alpha=0.99$					$\alpha=0.999$	$\alpha=0.99$
1	0.10	113.50	113.6	65.44	65.19	16	7.60	106.00	113.6	64.81	64.79
2	0.60	113.00	113.6	65.37	65.13	17	8.10	105.50	113.6	64.87	64.80
3	1.10	112.50	113.6	65.30	65.08	18	8.60	105.00	113.6	64.88	64.82
4	1.60	112.00	113.6	65.23	65.01	19	9.10	104.50	113.6	64.91	64.83
5	2.10	111.50	113.6	65.16	64.95	20	9.60	104.00	113.6	64.92	64.85
6	2.60	111.00	113.6	65.09	64.88	21	10.10	103.50	113.6	64.92	64.86
7	3.10	110.50	113.6	65.01	64.82	22	10.60	103.00	113.6	64.94	64.88
8	3.60	110.00	113.6	64.81	64.79	23	11.10	102.50	113.6	64.96	64.90
9	4.10	109.50	113.6	64.81	64.79	24	11.60	102.00	113.6	64.96	64.91
10	4.60	109.00	113.6	64.81	64.79	25	12.10	101.50	113.6	65.10	64.96
11	5.10	108.50	113.6	64.81	64.79	26	12.60	101.00	113.6	65.17	65.02
12	5.60	108.00	113.6	64.81	64.79	27	13.10	100.50	113.6	65.24	65.08
13	6.10	107.50	113.6	64.81	64.79	28	13.60	100.00	113.6	65.31	65.14
14	6.60	107.00	113.6	64.81	64.79	29	14.10	99.50	113.6	65.38	65.20
15	7.10	106.50	113.6	64.81	64.79						

707

708 **Figure captions**

709 **Fig. 1.** Flowchart of proposed method.

710 **Fig. 2.** Sketch of the two types for the two-reservoir system.

711 **Fig. 3.** Location of the Hanjiang basin and gauge stations.

712 **Fig. 4.** Relationship between flood storage of the two reservoirs and $CVaR_\alpha$ values:
713 (a) Three-dimensional perspective; (b) Projection to the $V_{DJK}-CVaR_\alpha$; (c) Projection
714 to the $V_{AK}-CVaR_\alpha$.

715 **Fig. 5.** Results of Scenario 1: the total flood storage of the Ankang-Danjiangkou multi-
716 reservoir system during the summer flood season is fixed at a constant value (i.e., 11.36
717 billion m^3), and then the FSCSs of the two reservoirs changes.

718 **Fig. 6.** Results of the feasible area for the FSCSs in the multi-reservoir system when
719 the total flood storage value ranges from 10.95 to 11.36 billion m^3 .

720 **Fig. 7.** Results of the $CVaR_{HZ,\alpha}$ values for the multi-reservoir system during the
721 summer flood season: (a) when the total flood storage value V changes from 10.95 to
722 15.13 billion m^3 ; (b) when the total flood storage value is fixed at 11.67 billion m^3 ; (c)
723 when the total flood storage value is fixed at 12.17 billion m^3 .

724 **Fig. 8.** Schematic diagram of feasible FLWLs/FSCSs area.

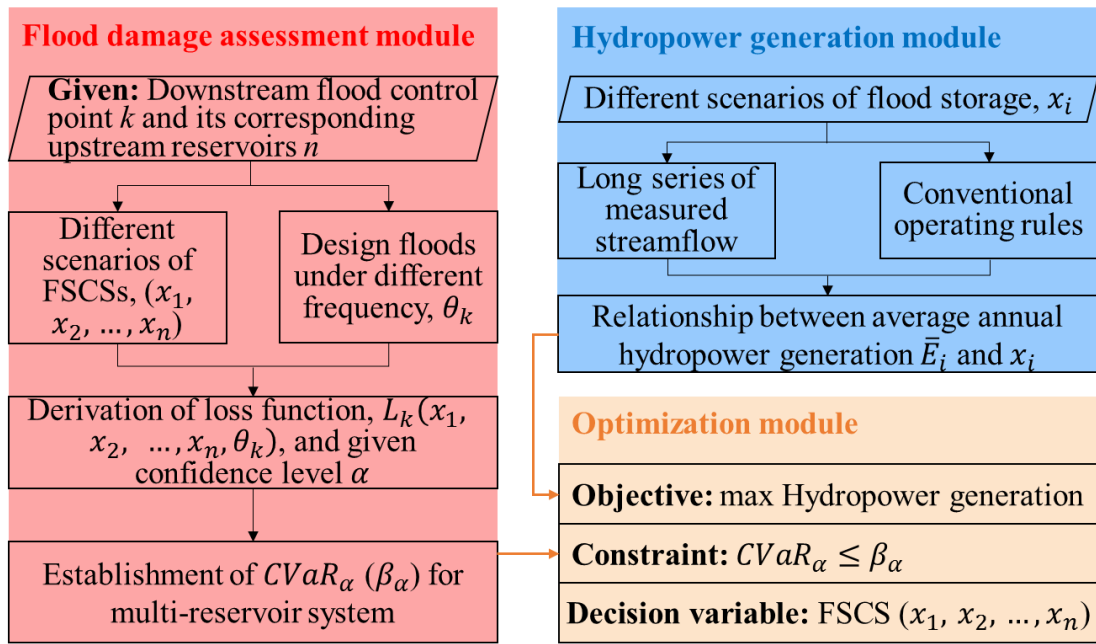
725 **Fig. 9.** Results of Scenario 2: the flood storage of the Ankang/Danjiangkou reservoir
726 changes while another reservoir's flood storage is fixed at its the present designed value.

727 **Fig. 10.** Optimal result when the total flood storage value is fixed at 11.36 billion m^3 .

728 **Fig. 11.** Optimal results when the total flood storage value V is successively fixed in
729 the range of 10.95 billion m^3 to 13.95 billion m^3 : (1) The solid lines in the horizontal
730 plane represent the different FSCSs, and the circle on each solid line is the optimal
731 FSCS when the term V is fixed at a constant value; (2) The asterisk points are the
732 vertical projection for the curved surface when the Ankang Reservoir's flood storage is
733 fixed at 0.36 billion m^3 .

734 **Fig. B1.** Schematic diagram of the location for the five reservoirs.

735 **Fig. B2.** Results of relationship between the flood damage assessment index $CVaR_\alpha$
736 value and Pankou/Sanliping/Yahekou reservoir's flood storage value.



738

739

Fig. 1. Flowchart of proposed method.

740

741

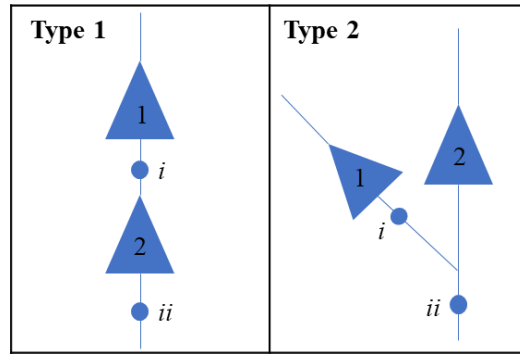
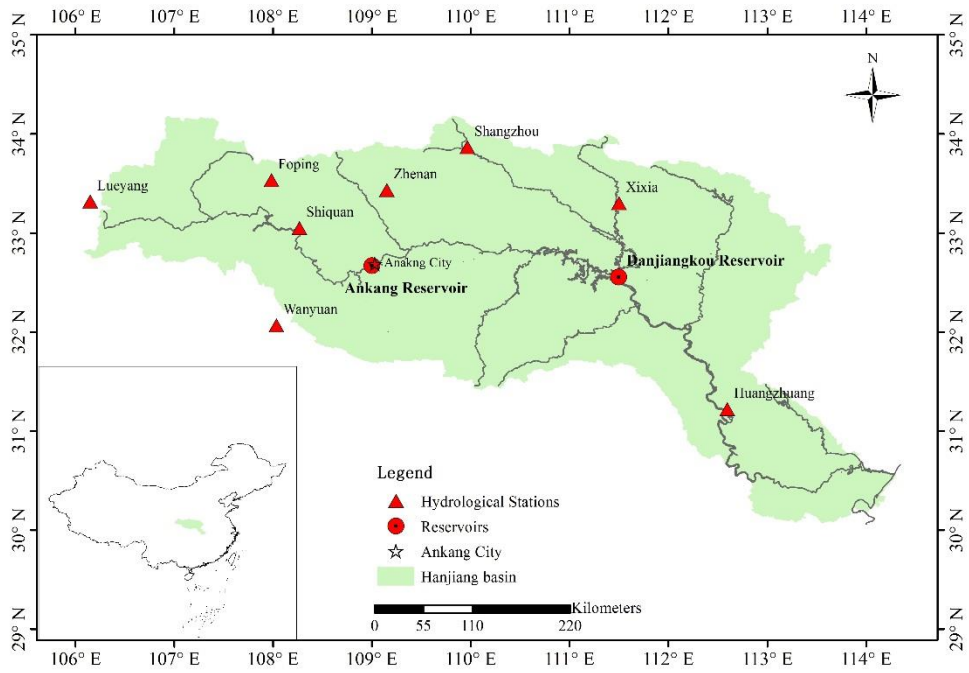


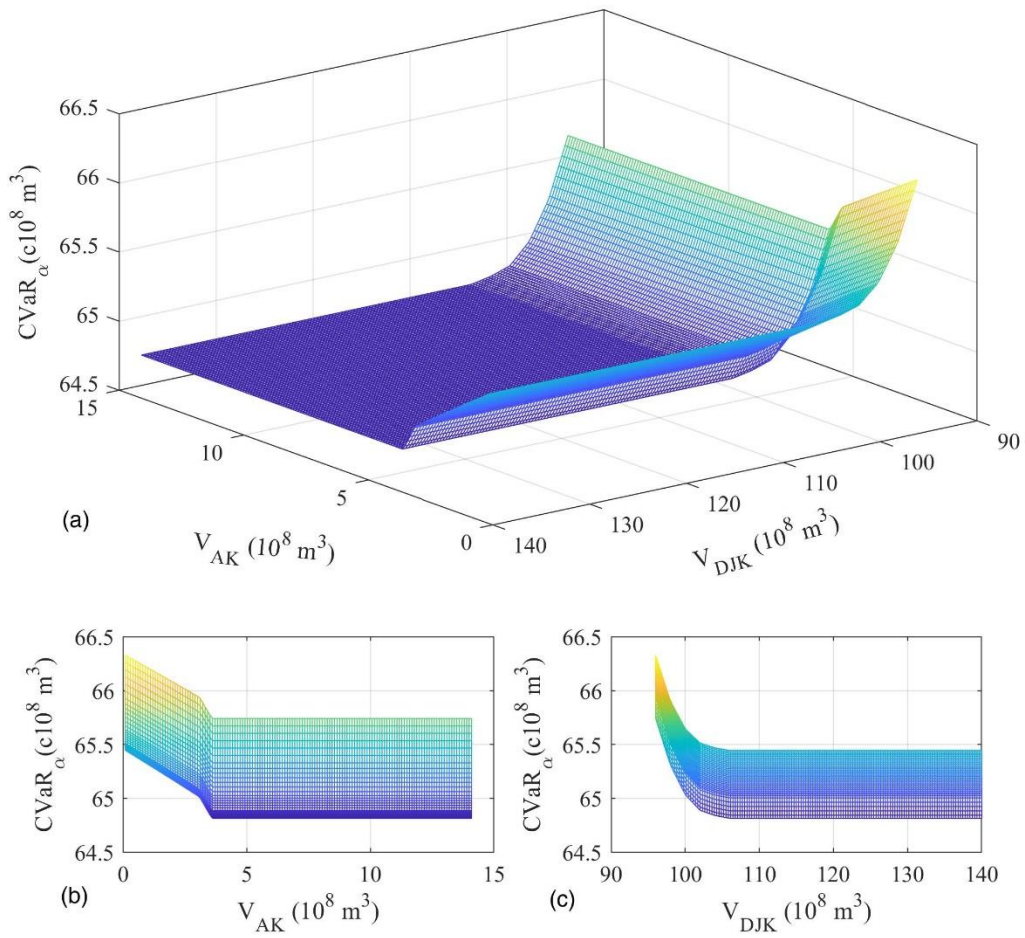
Fig. 2. Sketch of the two types for the two-reservoir system.



742

743

Fig. 3. Location of the Hanjiang basin and gauge stations.

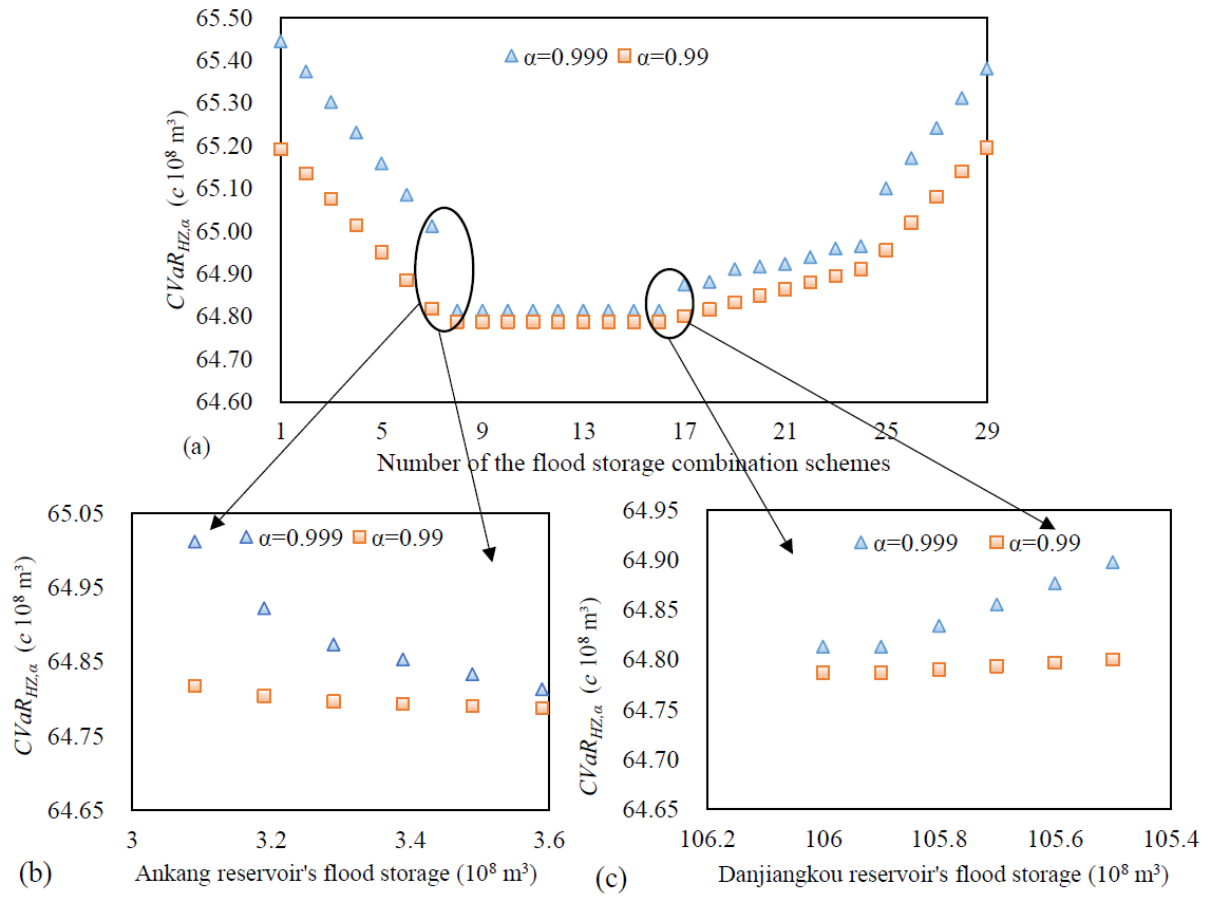


744

745 **Fig. 4.** Relationship between flood storage of the two reservoirs and $CVaR_\alpha$ values:

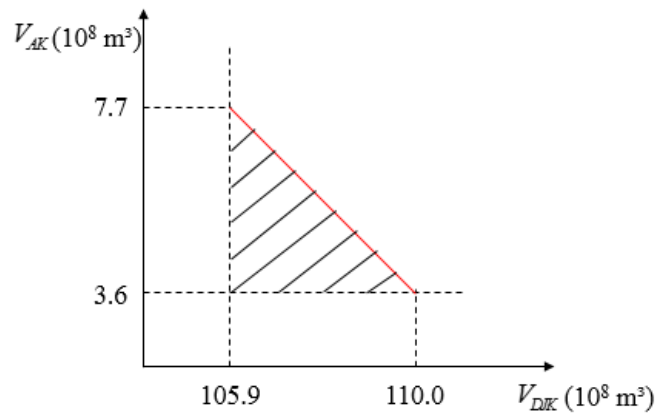
746 (a) Three-dimensional perspective; (b) Projection to the V_{DJK} - $CVaR_\alpha$; (c) Projection

747 to the V_{AK} - $CVaR_\alpha$.



748

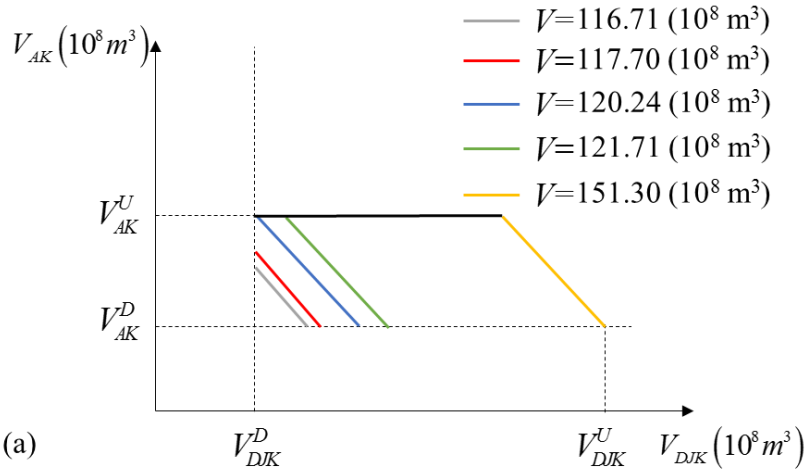
749 **Fig. 5.** Results of Scenario 1: the total flood storage of the Ankang-Danjiangkou multi-
 750 reservoir system during the summer flood season is fixed at a constant value (i.e., 11.36
 751 billion m³), and then the FSCSs of the two reservoirs changes.



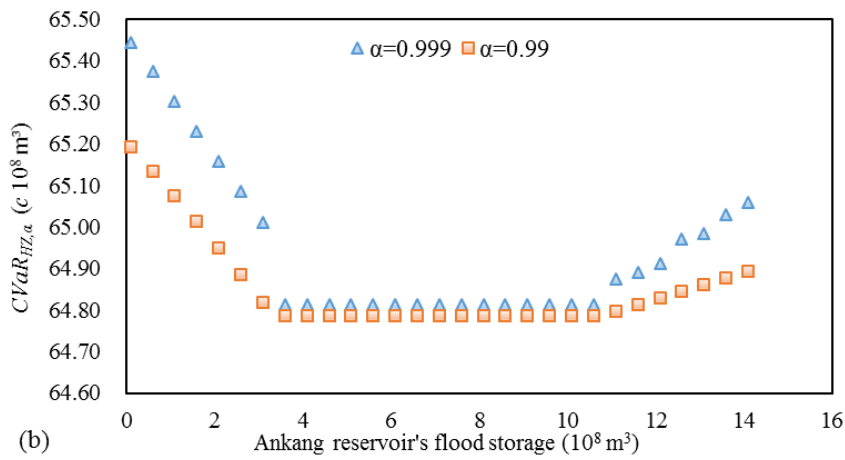
752

753 **Fig. 6.** Results of the feasible area for the FSCs in the multi-reservoir system when

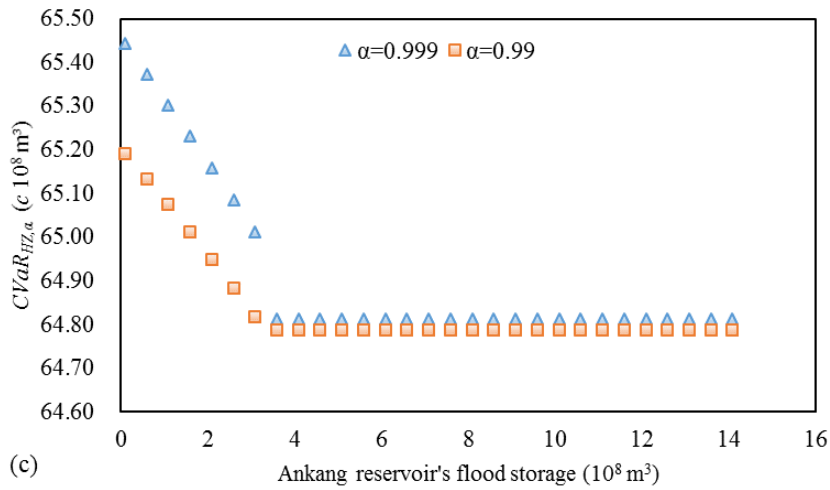
754 the total flood storage value ranges from 10.95 to 11.36 billion m^3 .



755

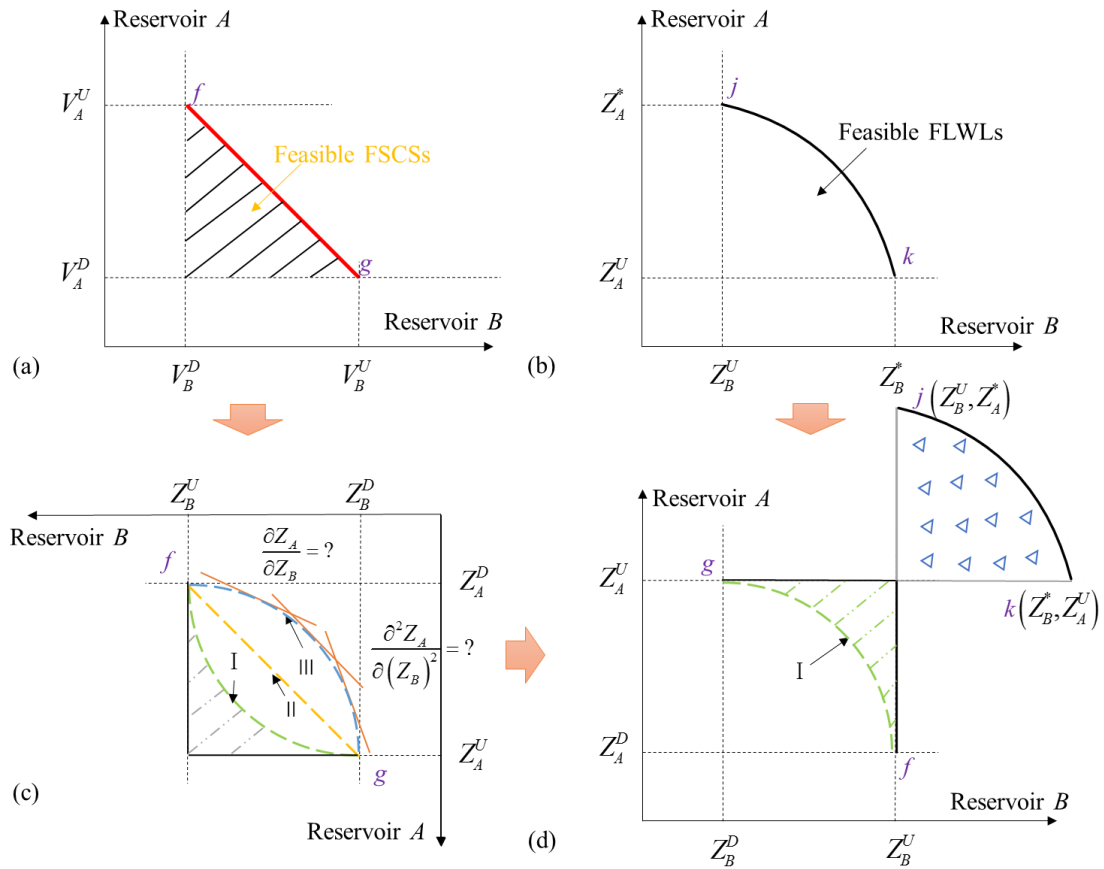


756



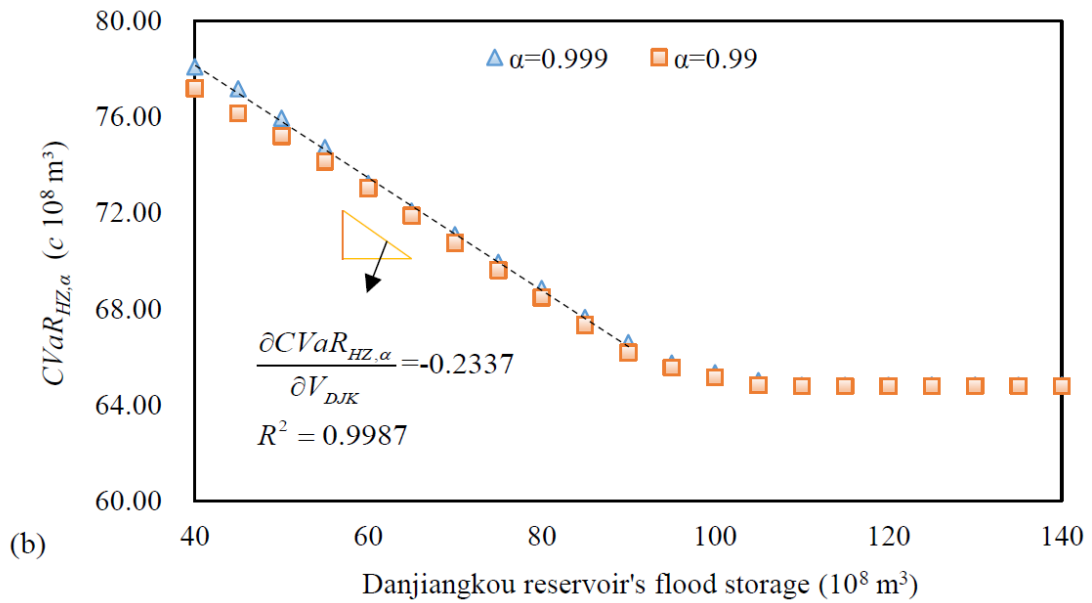
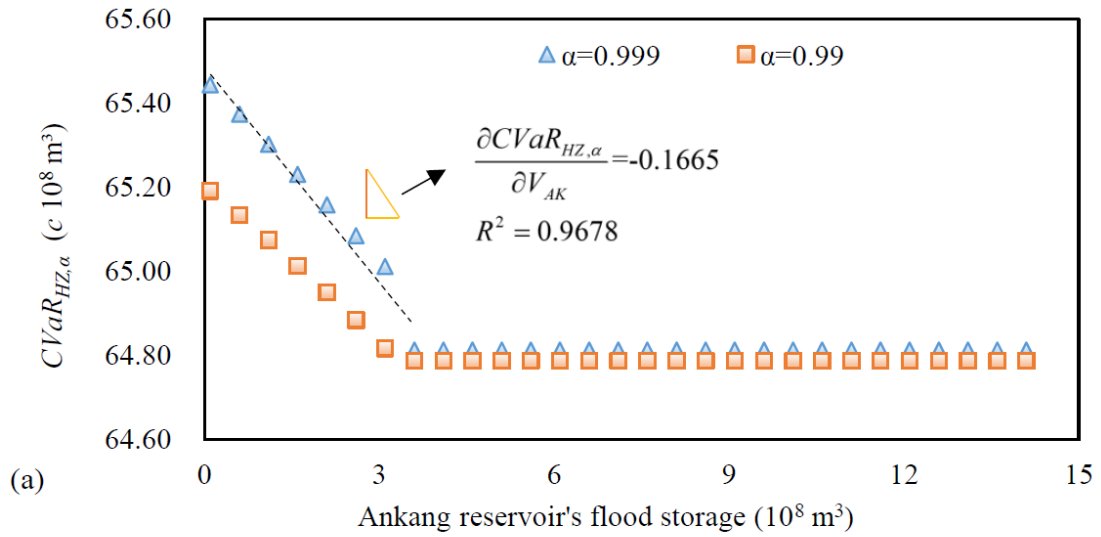
757

758 **Fig. 7.** Results of the $CVaR_{HZ,\alpha}$ values for the multi-reservoir system during the
 759 summer flood season: (a) when the total flood storage value V changes from 10.95 to
 760 15.13 billion m^3 ; (b) when the total flood storage value is fixed at 11.67 billion m^3 ; (c)
 761 when the total flood storage value is fixed at 12.17 billion m^3 .



762

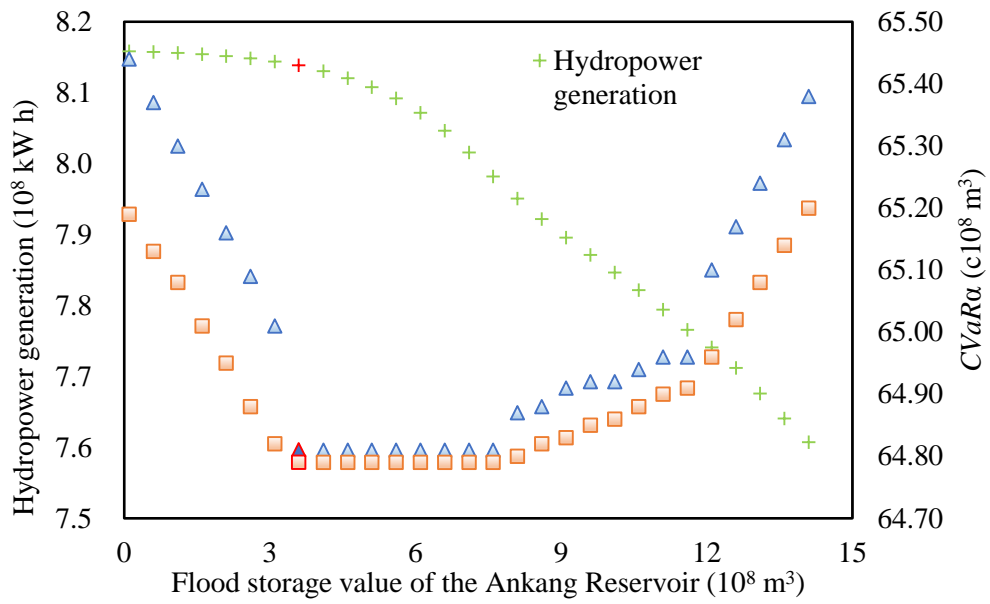
763 **Fig. 8.** Schematic diagram of feasible FLWLs/FSCSs area.



764

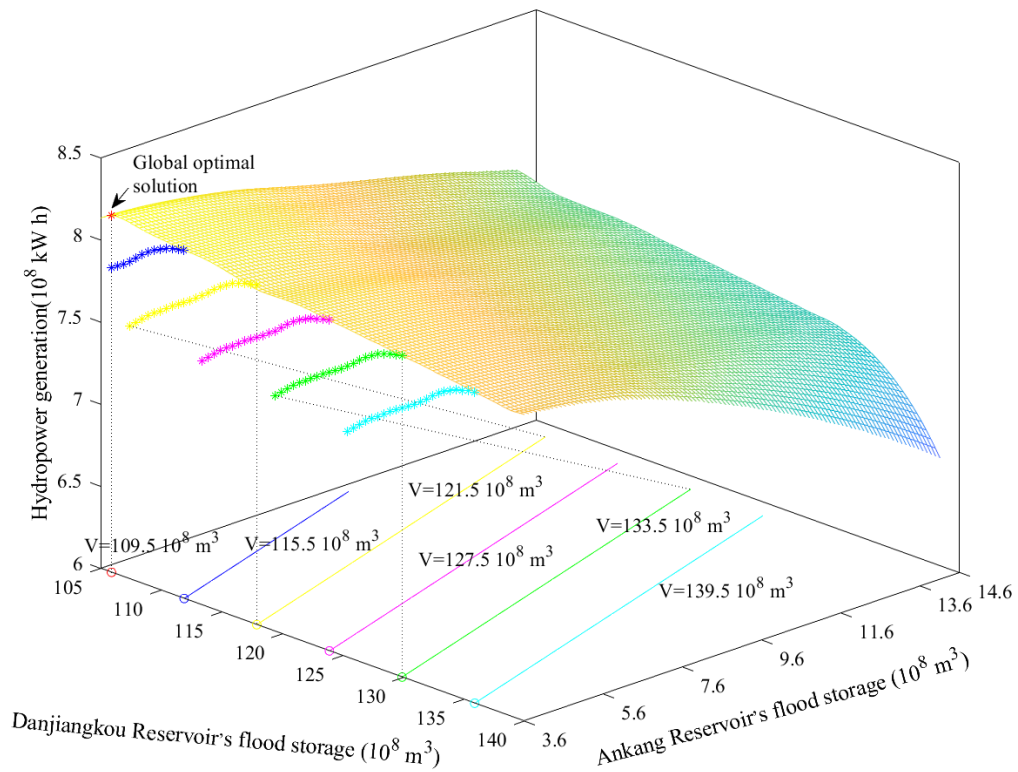
765 **Fig. 9.** Results of Scenario 2: the flood storage of the Anhang/Danjiangkou reservoir

766 changes while another reservoir's flood storage is fixed at its the present designed value.



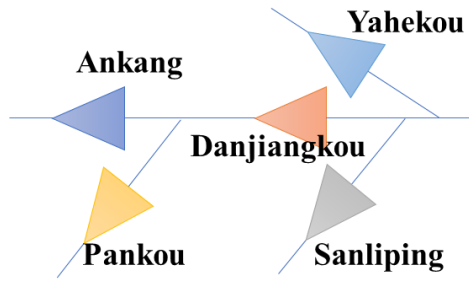
767

768 **Fig. 10.** Optimal result when the total flood storage value is fixed at 11.36 billion m^3 .



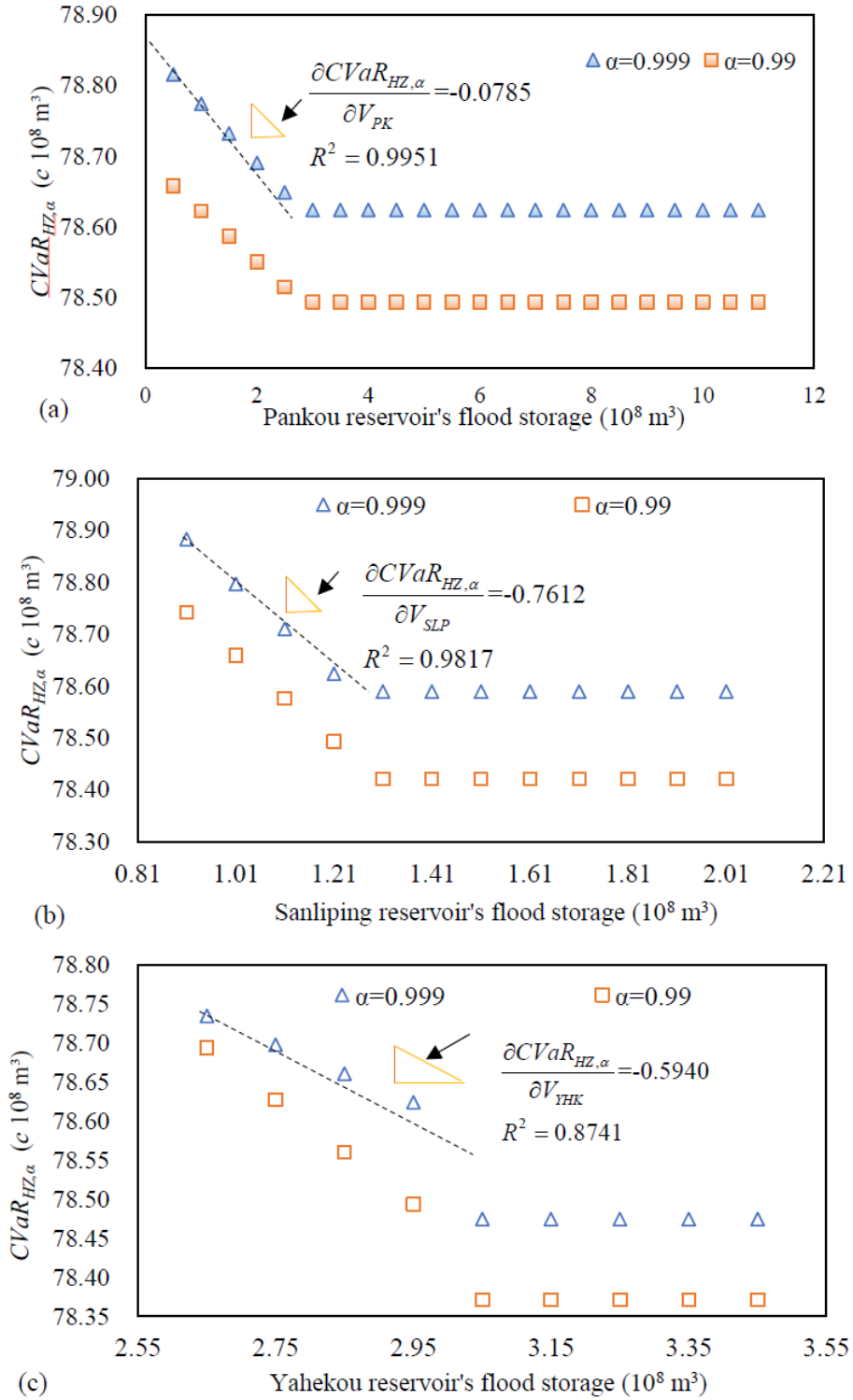
769

770 **Fig. 11.** Optimal results when the total flood storage value V is successively fixed in
 771 the range of 10.95 billion m^3 to 13.95 billion m^3 : (1) The solid lines in the horizontal
 772 plane represent the different FSCSs, and the circle on each solid line is the optimal
 773 FSCS when the term V is fixed at a constant value; (2) The asterisk points are the
 774 vertical projection for the curved surface when the Ankang Reservoir's flood storage is
 775 fixed at 0.36 billion m^3 .



776
777

Fig. B1. Schematic diagram of the location for the five reservoirs.



778

779 **Fig. B2.** Results of relationship between the flood damage assessment index $CVaR_{\alpha}$

780 value and Pankou/Sanliping/Yahekou reservoir's flood storage value.

Declaration of interests

The authors declare that they have no known competing financial interests or personal relationships that could have appeared to influence the work reported in this paper.

The authors declare the following financial interests/personal relationships which may be considered as potential competing interests:

Author statement

Zhang Xiaoqi: Conceptualization, Methodology, Software Writing- Original Draft
Liu Pan: Conceptualization, Supervision, Writing- Review & Editing
Feng Maoyuan: Methodology, Validation, Writing- Review & Editing
Xu Chong-Yu: Supervision, Writing- Review & Editing
Cheng Lei: Validation, Writing- Review & Editing
Gong Yu: Data Curation, Writing- Review & Editing